Inorg. Chem. **2008**, *47*, 11417−11422

Cleavage of the Indium(III) Octaethyloxophlorin Dimer, $\{In^{III}(OEPO)\}_2$, with Lewis Bases. Importance of Outer-Sphere Hydrogen Bonding in Adduct Structures

Thelma Y. Garcia, Marilyn M. Olmstead, James C. Fettinger, and Alan L. Balch*

Department of Chemistry, University of California, Davis, California 95616

Received August 22, 2008

Splitting of the oxygen-bridged dimer $\{In^{III}(OEPO)\}_2$ [where $(OEPO)^{3-}$ is the trianion of octaethyloxophlorin] by potential axial ligands has been examined and compared to results obtained previously for the cleavage of $\{Fe^{III}(OEPO)\}_2$. Treatment of $\{In^{III}(OEPO)\}_2$ with an excess of imidazole (im) produced the crystalline complex $\{(im)_2In^{III}(OEPO\cdots im)\}_2\cdot(im)_2In^{III}(OEPO)\cdot 2Cl_2C_6H_4$. This solid contains two different $(im)_2In^{III}(OEPO)$ units that are bridged through hydrogen bonding by an uncoordinated imidazole. Treatment of $\{In^{III}(OEPO)\}_2$ with an excess of pyridine (py) produced $(py)_2In^{III}(OEPO)$, which is isostructural with $(py)_2Fe^{III}(OEPO)$. Although $\{Fe^{III}(OEPO)\}_2$ reacted with xylyl isocyanide (xylylNC) to form the novel free-radical complex $(2,6\text{-xylylNC})_2Fe^{II}(OEPO^{\bullet})$ [where $(OEPO^{\bullet})^{2-}$ is the radical dianion of octaethyloxophlorin], $\{In^{III}(OEPO)\}_2$ was unreactive toward xylyl isocyanide.

Introduction

As seen in Scheme 1, the oxophlorin and *meso*-hydroxyporphyrin macrocycles exist in tautomeric equilibrium.[1] Iron complexes of *meso*-hydroxyporphyrin are intermediates in the ring-opening reactions of heme that are involved in its oxidative destruction either by coupled oxidation[2] or by the enzyme heme oxygenase.[3] Defining the electronic structure of such meso-hydroxylated iron porphyrins is a complex issue because there is a need to ascertain the oxidation states of both the ligand and the iron ion.[1,4] In that regard, the electronic structure of $(py)_2Fe(OEPO)$ [where $(OEPO)^{3-}$ is the trianion of octaethyloxophlorin] has received considerable attention.[5−10] Dark-blue crystals of $(py)_2Fe(OEPO)$ and related adducts are readily obtained through the reaction of $\{Fe^{III}(OEPO)\}_2$ with the appropriate axial ligand, as shown in Scheme 2. In the solid state, recent results have shown that complexes of the type $(py)_2Fe(OEPO)$ (L = pyridine, imidazole, and *N*-methylimidazole) exist in the iron(III)/oxophlorin trianion form[9,10] rather than the iron(II)/oxophlorin radical form that was previously established for $(2,6\text{-xylylNC})_2Fe^{II}(OEPO^{\bullet})$.[9] The π-accepting isocyanide ligands play a key role in stabilizing the low-spin Fe^{II} oxidation state in $(2,6\text{-xylylNC})_2Fe^{II}(OEPO^{\bullet})$. In solution, $(py)_2Fe(OEPO)$ (L = pyridine, imidazole, and *N*-methylimidazole) and $(2,6\text{-xylylNC})_2Fe^{II}(OEPO^{\bullet})$ are extremely air-sensitive and undergo conversion into verdohemes when exposed to dioxygen.[11,12]

This Article explores the axial coordination of indium octaethyloxophlorin in order to provide further insight into the electronic properties of the oxophlorin ligand ion in its complexes. In porphyrin complexes, indium usually exists as In^{III}, while the In^{II} and In^{I} states are extremely unlikely to be observed because indium is a main-group element rather than a transition metal. Indium does form $\{In^{III}(OEPO)\}_2$,[13] whose structure is analogous to that of $\{Fe^{III}(OEPO)\}_2$.[14] Both $\{In^{III}(OEPO)\}_2$ and $\{Fe^{III}(OEPO)\}_2$ have been characterized by single-crystal X-ray diffraction.[13,14] By analogy with the behavior of $\{Fe^{III}(OEPO)\}_2$, we

* To whom correspondence should be addressed. E-mail: albalch@ucdavis.edu.

(1) Balch, A. L. *Coord. Chem. Rev.* **2000**, *200*−*202*, 349.
(2) St. Claire, T. N.; Balch, A. L. *Inorg. Chem.* **1999**, *38*, 684.
(3) Ortiz de Montellano, P. R. *Acc. Chem. Res.* **1998**, *31*, 543.
(4) Szterenberg, L.; Latos-Grazynski, L.; Wojaczynski, J. *ChemPhysChem* **2002**, *3*, 575.
(5) Sano, S.; Suigura, Y.; Maeda, Y.; Ogawa, S.; Morishima, I. *J. Am. Chem. Soc.* **1981**, *103*, 2888.
(6) Sano, S.; Sano, T.; Morishima, I.; Shiro, Y.; Maeda, Y. *Proc. Natl. Acad. Sci. U.S.A.* **1986**, *83*, 531.
(7) Morishima, I.; Fujii, H.; Shiro, Y. *J. Am. Chem. Soc.* **1986**, *108*, 3858.
(8) Balch, A. L.; Koerner, R.; Latos-Grazynski, L.; Noll, B. C. *J. Am. Chem. Soc.* **1996**, *118*, 2760.
(9) Rath, S. P.; Olmstead, M. M.; Balch, A. L. *J. Am. Chem. Soc.* **2004**, *126*, 6379.
(10) Rath, S. R.; Olmstead, M. M.; Balch, A. L. *Inorg. Chem.* **2006**, *45*, 6083.
(11) Balch, A. L.; Latos-Grazynski, L.; Noll, B. C.; Olmstead, M. M.; Szterenberg, L.; Safari, N. *J. Am. Chem. Soc.* **1993**, *115*, 1422.
(12) Rath, S. P.; Olmstead, M. M.; Balch, A. L. *Inorg. Chem.* **2004**, *43*, 7648.

10.1021/ic801605b CCC: $40.75
Published on Web 10/25/2008

Scheme 1. Tautomeric Equilibrium between *meso*-Hydroxyporphyrin and Oxophlorin

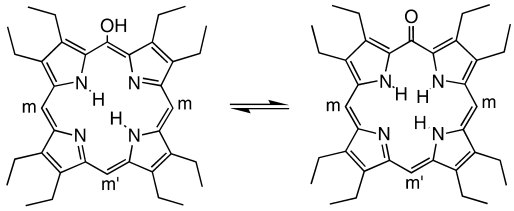

anticipated that suitable Lewis bases would be able to cleave this dimer and add to the indium. However, we also were aware that ClIn^{III}(OEP) has been shown to be unreactive toward coordination of either pyridine or *N*-methylimidazole.[15] Moreover, there are no six-coordinate indium porphyrin complexes reported in the Cambridge Crystallographic Database.[16]

Results

Interactions of {In^{III}(OEPO)}$_2$ with Lewis Bases. Preparative details for the formation of {In^{III}(OEPO)}$_2$, which follow those briefly outlined earlier,[13] are given in the Experimental Section. The reactions between {In^{III}(OEPO)}$_2$ and Lewis bases have been monitored by both UV/vis and ^{1}H NMR spectroscopy. These reactions can be performed in the presence of dioxygen because the products, unlike their iron counterparts, are air-stable. Trace A of Figure 1 shows the UV/vis spectrum of {In^{III}(OEPO)}$_2$ in a dichloromethane solution. This spectrum is similar to that of {Fe^{III}(OEPO)}$_2$ reported earlier.[4,17] Trace B of Figure 1 shows the UV/vis spectrum of (im)$_2$In^{III}(OEPO), which was obtained by the addition of an excess of imidazole to a solution of {In^{III}(OEPO)}$_2$. Trace C shows the spectrum (py)$_2$In^{III}(OEPO), which was prepared by the addition of an excess of pyridine to a dichloromethane solution of {In^{III}(OEPO)}$_2$. The spectra of both of these adducts are similar and clearly distinct from that of their precursor, {In^{III}(OEPO)}$_2$. For (py)$_2$In^{III}(OEPO) and (im)$_2$In^{III}(OEPO), there are intense absorptions at ca. 690 nm, which are similar to the low-energy absorption at 662 nm found in the absorption spectrum of (2-Me-im)$_2$Fe^{III}(OEPO).[10] However, there was no change in the UV/vis spectrum of {In^{III}(OEPO)}$_2$ when it was treated with an excess of xylyl isocyanide.

^{1}H NMR spectra also show that imidazole and pyridine cleave {In^{III}(OEPO)}$_2$ to form monomeric adducts, as shown in Scheme 3. The ^{1}H NMR spectrum of {In^{III}(OEPO)}$_2$ in chloroform-*d* consists of a characteristic set of four equally intense methyl triplets at 0.02 ppm (6H; J = 7.8 Hz), 1.44 ppm (6H; J = 7.8 Hz), 2.00 ppm (6H; J = 7.8 Hz), and 2.05 ppm (6H; J = 7.7 Hz). These resonances are shown in trace A of Figure 2. Note that two methyl groups at 0.02 and 1.44 ppm have experienced significant upfield shifts. These shifts, which are the result of the ring current on the neighboring macrocycle, allow us to assign these resonances to ^{a}Et and ^{b}Et, respectively, in Scheme 3. The methylene region is complex. Sextets occur at 1.86 and 3.88 ppm because of the two environmentally distinct methylene protons of the ethyl group (^{a}Et in Scheme 3) that is adjacent to the oxygen atom. The sextet pattern with a 1:3:4:4:3:1 intensity ratio results from the presence of two overlapping methylene quartets in which the two inequivalent methylene protons split from one another. This ethyl group lies in the face of the adjacent macrocycle, and its resonances are shifted upfield by the ring current of the neighboring π system. The methylene protons of ethyl groups—^{b}Et, ^{c}Et, and ^{d}Et—produce a complex multiplet between 4.02 and 4.13 ppm. Singlet resonances at 10.11 ppm (2H) and 9.96 ppm (1H) are assigned to the meso protons.

The addition of pyridine-d_5 to a dichloromethane-d_2 solution of {In^{III}(OEPO)}$_2$ results in the loss of resonances of the dimer as described above and the creation of new resonances due to (py)$_2$In^{III}(OEPO). A similar spectrum is obtained when {In^{III}(OEPO)}$_2$ is dissolved in pyridine. Traces B and C in Figure 2 show the characteristic methyl resonances of (py)$_2$In^{III}(OEPO). The ^{1}H NMR spectrum of (py)$_2$In^{III}(OEPO) in pyridine-d_5 consists of methyl triplets at 1.62 ppm (6H; J = 7.8 Hz), 1.64 ppm (12H; J = 7.8 Hz), and 1.92 ppm (6H; J = 7.8 Hz), methylene quartets at 3.48 ppm (4H; J = 7.8 Hz), 3.50 ppm (4H; J = 7.8 Hz), 3.63 ppm (4H; J = 7.8 Hz), and 4.11 ppm (4H; J = 7.8 Hz) and meso resonances at 8.94 ppm (2H) and 8.33 ppm (1H). This pattern is fully consistent with splitting of the dimer, {In^{III}(OEPO)}$_2$, to form a symmetric monomer that no longer exhibits the upfield-shifted methyl resonances that are characteristic of the ring current effects in the overlapped dimer. In contrast, when excess xylyl isocyanide is added to a chloroform-*d* solution of {In^{III}(OEPO)}$_2$, the spectrum of the dimer remains unaltered. Thus, the ^{1}H NMR results confirm the conclusion derived from the UV/vis measurements: there is no evidence for a reaction between {In^{III}(OEPO)}$_2$ and xylyl isocyanide.

Structure and Hydrogen-Bonding Interactions of {(im)$_2$-In^{III}(OEPO···im)}$_2$·(im)$_2$In^{III}(OEPO)·2Cl$_2$C$_6$H$_4$. Crystals of this adduct were obtained from a green solution of {In^{III}(OEPO)}$_2$ and excess imidazole in 1,2-dichlorobenzene. Crystal data are given in Table 1. The asymmetric unit consists of half of the hydrogen-bonded aggregate {(im)$_2$-In^{III}(OEPO···im)}$_2$ in a general position, half of a molecule of (im)$_2$In^{III}(OEPO) with the indium atom located on a center of symmetry, and one molecule of *o*-dichlorobenzene in a general position.

Figure 3 shows a drawing of the structure of half of the {(im)$_2$In^{III}(OEPO···im)}$_2$ aggregate. Relevant bond distances and angles are given in the figure caption. The complex contains a six-coordinate indium ion with two axial imidazole ligands, which are aligned nearly perpendicularly to one another. The axial N5−In−N7 angle [174.77(14)°] is slightly

(13) Balch, A. L.; Noll, B. C.; Olmstead, M. M.; Reid, S. M. *J. Chem. Soc., Chem. Commun.* **1993**, 1088.
(14) Lee, H. M.; Olmstead, M. M.; Gross, G. G.; Balch, A. L. *Cryst. Growth Des.* **2003**, *3*, 691.
(15) Cornillon, J.-L.; erson, J. E.; Kadish, K. M. *Inorg. Chem.* **1986**, *25*, 991.
(16) Allen, F. H. *Acta Crystallogr.* **2002**, *B58*, 380.
(17) Balch, A. L.; Latos-Grazynski, L.; Noll, B. C.; Olmstead, M. M.; Zovinka, E. P. *Inorg. Chem.* **1992**, *31*, 2248.

Scheme 2. Reactions of $\{Fe^{III}(OEPO)\}_2$

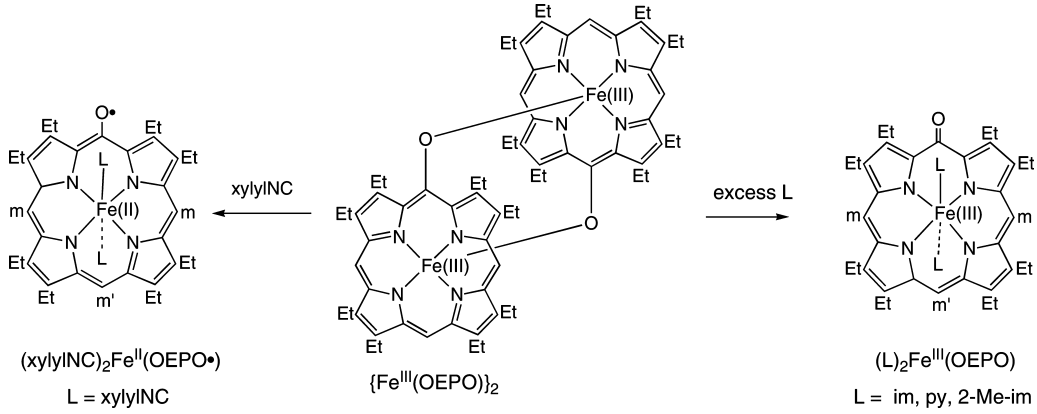

bent. The axial In−N bond lengths [2.298(5) and 2.331(5) Å] are significantly longer than the in-plane In−N distances [range: 2.120(4)−2.126(4) Å]. The in-plane In−N distances are similar to those seen in five-coordinate indium(III) porphyrins. For example, in five-coordinate (4-phenyltetrazolato)indium(III) octaethylporphyrin, the In−N(porphyrin) distances range from 2.130(6) to 2.140(7) Å, while the In−N(tetrazole) distance is slightly longer, 2.177(6) Å.[18] Another imidazole molecule acts as a hydrogen-bond donor to the oxygen atom on the periphery of the porphyrin. The O1−C5 bond distance [1.294(6) Å] is consistent with the presence of significant double-bond character, as expected for the oxophlorin formulation of the molecule.

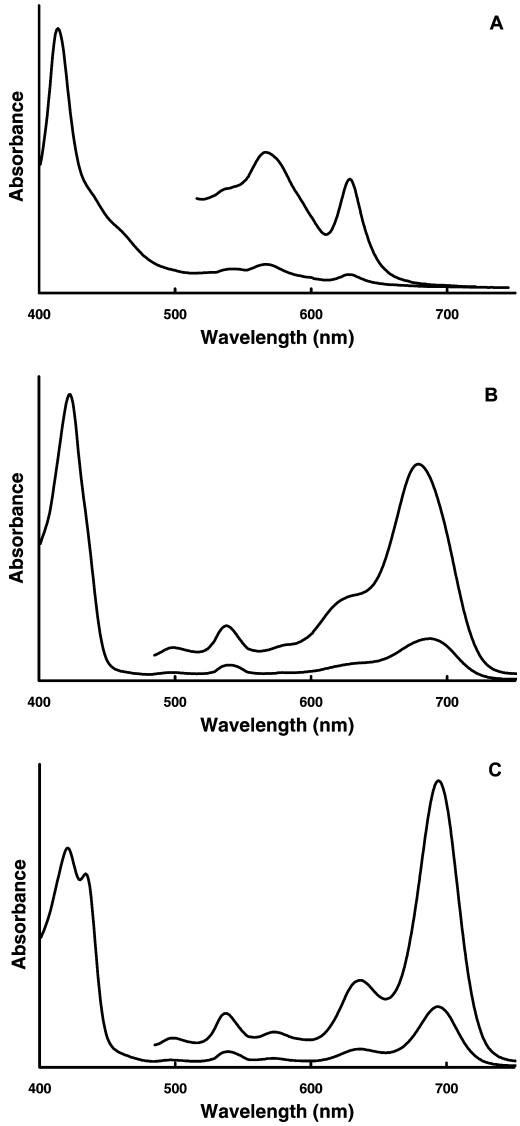

Figure 1. Electronic absorption spectra of (trace A) a solution of $\{In^{III}(OEPO)\}_2$ ($M = 2.8 \times 10^{-5}$) in dichloromethane, (trace B) $(py)_2In^{III}(OEPO)$ formed upon the addition of excess pyridine, and (trace C) $(im)_2In^{III}(OEPO)$ formed upon the addition of excess imidazole.

Figure 4 shows a drawing of the structure of the centrosymmetric $(im)_2In^{III}(OEPO)$ portion of the structure with some bond distances and angles given in the caption. Again the indium atom is six-coordinate with an axial In−N bond length [2.297(5) Å] that is longer than the in-plane In−N distances [2.129(4) and 2.141(4) Å]. In this molecule, the two axial ligands are oriented in parallel planes, a consequence of the crystallographic symmetry at this site. The meso oxygen atom, which does not participate in hydrogen bonding, is disordered over two centrosymmetrically related positions, each with 0.50 fractional occupancy. The C60−O60 distance is 1.279(11) Å, which is consistent with the presence of the $(OEPO)^{3-}$ form of the ligand.

Figure 5 shows the entire hydrogen-bonded aggregate $\{(im)_2In^{III}(OEPO\cdots im)\}_2$ and its relationship to the centrosymmetric $(im)_2In^{III}(OEPO)$ molecule. As this figure shows, the $(im)_2In^{III}(OEPO\cdots im)$ portion shown in Figure 3 dimerizes through two additional hydrogen bonds that involve the axial imidazole ligand of the indium complex acting as a hydrogen-bond donor toward the uncoordinated imidazole molecule. Thus, the uncoordinated imidazole bridges two indium complexes. This imidazole molecule acts as a hydrogen-bond donor to the oxygen atom of one indium complex and as a hydrogen-bond acceptor from one of the axial ligands of another indium complex. The ability of imidazole to hydrogen bond with itself has been noted previously.[19,20] The *o*-dichlorobenzene solvate molecule is situated to the side of the aggregate shown in Figure 4 and does not participate in hydrogen bonding with this aggregate.

Structure of $(py)_2In^{III}(OEPO)$. Dark-green needles of this complex were obtained by layering methanol over a solution

(18) Guilard, R.; Jagerovic, N.; Tabard, A.; Richard, P.; Courthaudon, L.; Louati, A.; Lecomte, C.; Kadish, K. M. *Inorg. Chem.* **1991**, *30*, 16.
(19) Doonan, D. J.; Balch, A. L. *J. Am. Chem. Soc.* **1975**, *97*, 1403.

Scheme 3. Reactions of $\{In^{III}(OEPO)\}_2$

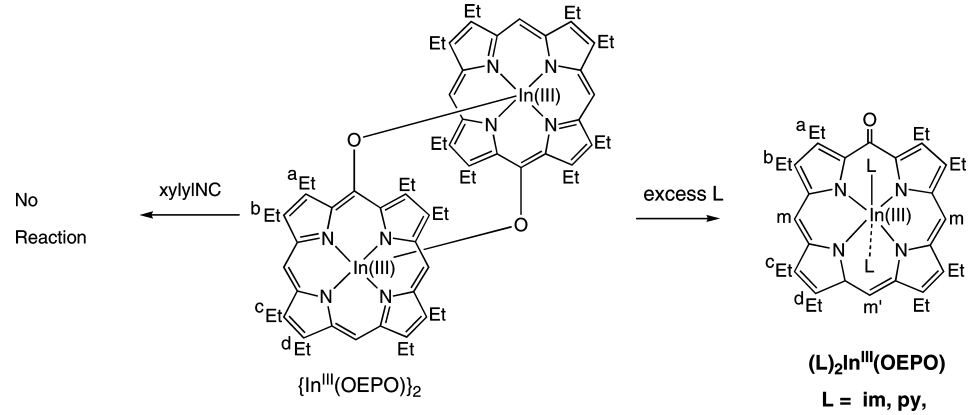

of $\{In^{III}(OEPO)\}_2$ and pyridine in chloroform. Crystals of $(py)_2In^{III}(OEPO)$ are isostructural with those of $(py)_2Fe^{III}(OEPO)$[8] and $(py)_2Mn^{III}(OEPO)$,[21] whose structures were reported earlier. The asymmetric unit consists of half of the molecule, with the indium ion located on a center of symmetry. Figure 6 shows the structure of the entire molecule, which closely resembles the centrosymmetric molecule of $(im)_2In^{III}(OEPO)$ shown in Figure 4. The indium atom is six-coordinate. The axial In−N bond length [2.4065(19) Å] is longer than the in-plane In−N distances [2.1203(18) and 2.1204(18) Å]. For comparison, in $(py)_2Fe^{III}(OEPO)$, the out-of-plane Fe−N distance, 2.2432(19) Å, is also longer than the in-plane Fe−N distances, 2.0476(18) and 2.0448(18) Å. However, in general, the In−N distances are longer than the Fe−N distances. The crystallographic symmetry requires that the two axial ligands are located in a common plane. The planes of these pyridine ligands are nearly coincident with the N1−In−N1A axis of the macrocycle. The oxygen atom does not participate in hydrogen bonding and is disordered so that there is an oxygen site with 0.25 fractional occupancy at each of the four molecular meso positions. The C5−O1A distance is 1.293(5) Å.

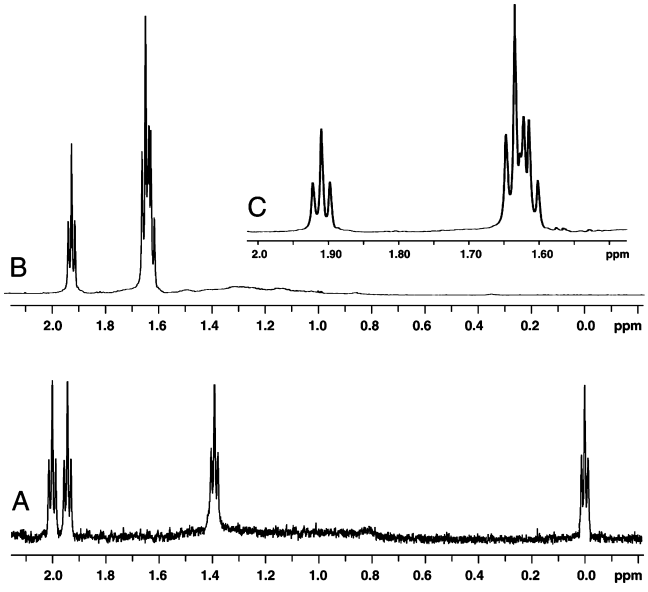

Figure 2. ^1H NMR spectra of the region of methyl resonances for (trace A) $\{In^{III}(OEPO)\}_2$ in chloroform-*d* and (trace B) $(py)_2In^{III}(OEPO)$ formed by dissolving $\{In^{III}(OEPO)\}_2$ in pyridine-d_5. The inset (trace C) shows an expansion of the 2.0−1.5 ppm region of the spectrum in B.

Table 1. Crystallographic Data

	$\{(im)_2In^{III}(OEPO\cdots im)\}_2\cdot$ $(im)_2In^{III}(OEPO)\cdot 2Cl_2C_6H_4$	$(py)_2In^{III}(OEPO)$
color/habit	dark-green plate	dark-green needle
formula	$C_{144}H_{169}Cl_4In_3N_{28}O_3$	$C_{46}H_{53}InN_6O$
fw	2826.33	820.76
cryst syst	triclinic	triclinic
space group	$P\bar{1}$	$P\bar{1}$
a, Å	14.8697(14)	9.8499(7)
b, Å	15.2718(15)	10.3078(7)
c, Å	15.7681(16)	10.4743(7)
α, deg	97.908(2)	80.364(2)
β, deg	99.977(2)	89.6920(10)
γ, deg	96.864(2)	65.9460(10)
V, Å^3	3455.1(6)	955.08(11)
Z	1	1
T, K	90(2)	90(2)
λ, Å	0.710 73	0.710 73
d_{calcd}, g/cm^3	1.358	1.427
μ, mm^{-1}	0.637	0.664
no. of unique data	12 494	5593
no. of restraints	0	0
no. of params refined	838	253
R1 (obsd data)	0.055	0.042
wR2 (all data)	0.154	0.089[a]

[a] For data with $I > 2\sigma(I)$, R1 = $(\sum||F_o| - |Fc||)/(\sum|F_o|)$. For all data, wR2 = $[(\sum[w(F_o^2 - F_c^2)^2])/(\sum[w(F_o^2)^2])]^{1/2}$.

Discussion

The results involving cleavage of $\{In^{III}(OEPO)\}_2$ by Lewis bases that are summarized in Scheme 3 indicate that $\{In^{III}(OEPO)\}_2$, unlike $ClIn^{III}(OEP)$, does rather readily react and add axial ligands to form six-coordinate complexes. $\{In^{III}(OEPO)\}_2$ is cleaved by imidazole or pyridine to form six-coordinate In^{III}-containing products that are stable to air. In the establishment of an analogy between the indium and iron chemistry, it is particularly significant that the products $(py)_2In^{III}(OEPO)$ and $(py)_2Fe^{III}(OEPO)$ are isostructural. Xylyl isocyanide cleaves $\{Fe^{III}(OEPO)\}_2$ to form the unusual free-radical complex $(2,6\text{-xylylNC})_2Fe^{II}(OEPO^{\bullet})$ that contains Fe^{II}.[9] The *π*-accepting character of the isocyanide ligand is a significant factor in stabilizing the Fe^{II} oxidation state of

(20) Joop, N. *Z. Elektrochem.* **1962**, *66*, 541.
(21) Balch, A. L.; Noll, B. C.; Reid, S. M.; Zovinka, E. P. *Inorg. Chem.* **1993**, *32*, 2610.

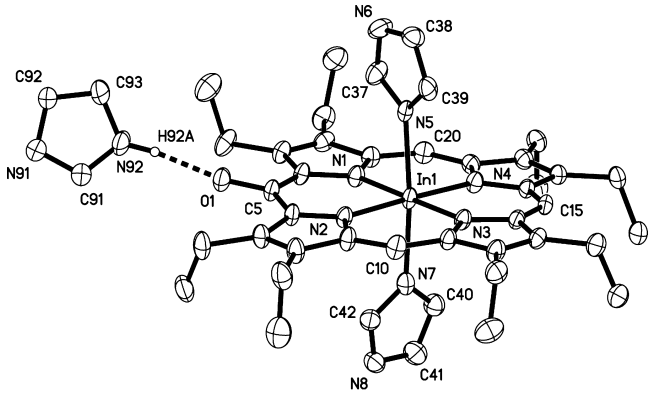

Figure 3. Drawing of half of the $\{(im)_2In^{III}(OEPO\cdots im)\}_2$ unit in $\{(im)_2In^{III}(OEPO\cdots im)\}_2\cdot(im)_2In^{III}(OEPO)\cdot 2Cl_2C_6H_4$ with 30% thermal contours. Hydrogen atoms are not shown. Selected bond distances (Å): In1−N1, 2.123(4); In1−N2, 2.126(4); In1−N3, 2.120(4); In1−N4, 2.120(4); In1−N5, 2.331(5); In1−N7, 2.298(5); O1−C5, 1.294(6). Selected bond angles (deg): N1−In1−N5, 87.24(16); N2−In1−N5, 89.43(16); N3−In1−N5, 92.27(16); N4−In1−N5, 92.53(16); N1−In1−N7, 88.49(16); N2−In1−N7, 87.50(17); N3−In1−N7, 92.00(16); N4−In1−N7, 90.55(17); N7−In1−N5, 174.77(14).

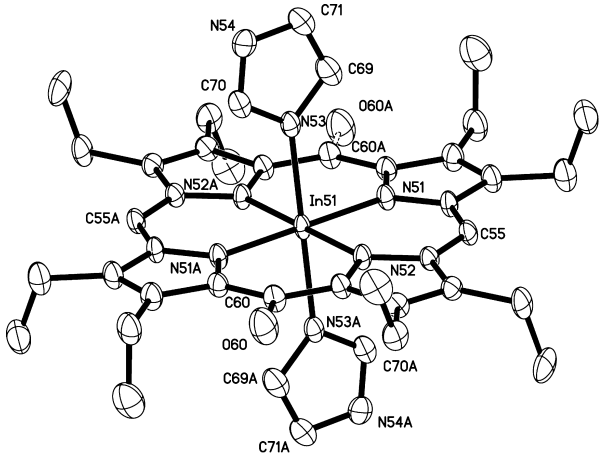

Figure 4. Drawing of the centrosymmetric $(im)_2In^{III}(OEPO)$ molecule (with 30% thermal contours) in $\{(im)_2In^{III}(OEPO\cdots im)\}_2\cdot(im)_2In^{III}(OEPO)\cdot 2Cl_2C_6H_4$. Hydrogen atoms are not shown. Selected bond distances (Å): In51−N51, 2.129(4); In51−N52, 2.141(4); In51−N53, 2.297(5); C60−O60, 1.279(11).

iron in this free-radical complex. In contrast, $\{In^{III}(OEPO)\}_2$ is unreactive toward xylyl isocyanide because it cannot form an analogous indium(II) compound.

With the $(OEPO)^{3-}$ ligand, the oxygen atom is buried within the bulk of the peripheral ethyl substituents and, by itself, has a relatively minor effect on the external shape of the ligand. Consequently, this ligand is prone to disorder. The structures of $\{(im)_2In^{III}(OEPO\cdots im)\}_2\cdot(im)_2In^{III}(OEPO)\cdot 2Cl_2C_6H_4$ and $(py)_2In^{III}(OEPO)$ demonstrate the importance of hydrogen bonding in producing ordered structures of the $(OEPO)^{3-}$ ligand. In the former, the $In^{III}(OEPO)$ moiety in the hydrogen-bonded aggregate $\{(im)_2In^{III}(OEPO\cdots im)\}_2$ is ordered, while the centrosymmetric $(im)_2In^{III}(OEPO)$ unit lacks hydrogen bonding to the meso oxygen atoms and is, as a consequence, disordered. In $(py)_2In^{III}(OEPO)$, the meso oxygen atoms do not participate in hydrogen bonding and the $(OEPO)^{3-}$ moiety is disordered, as it is in $(py)_2Fe^{III}(OEPO)$.

Hydrogen bonding to coordinated imidazole ligands is a topic of current interest. For example, in heme proteins,

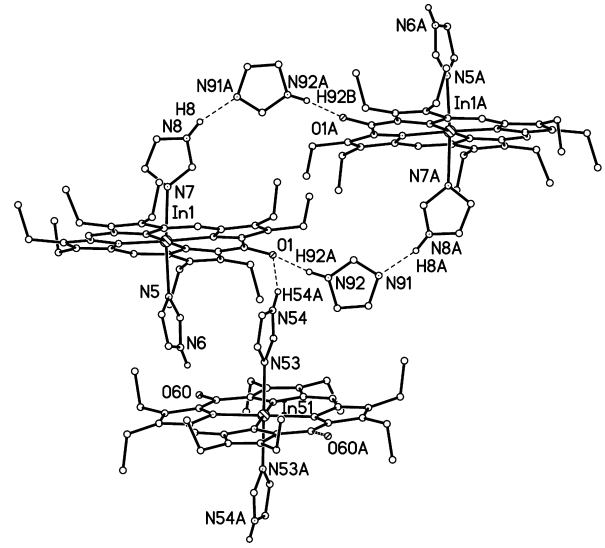

Figure 5. Drawing of the interactions between the hydrogen-bonded aggregate $\{(im)_2In^{III}(OEPO\cdots im)\}_2$ and the centrosymmetric $(im)_2In^{III}$-(OEPO) molecule in $\{(im)_2In^{III}(OEPO\cdots im)\}_2\cdot(im)_2In^{III}(OEPO)\cdot 2Cl_2C_6H_4$. For clarity, atoms are represented by arbitrarily sized circles and the solvate molecules are not shown. Only those hydrogen atoms involved in hydrogen bonding are shown.

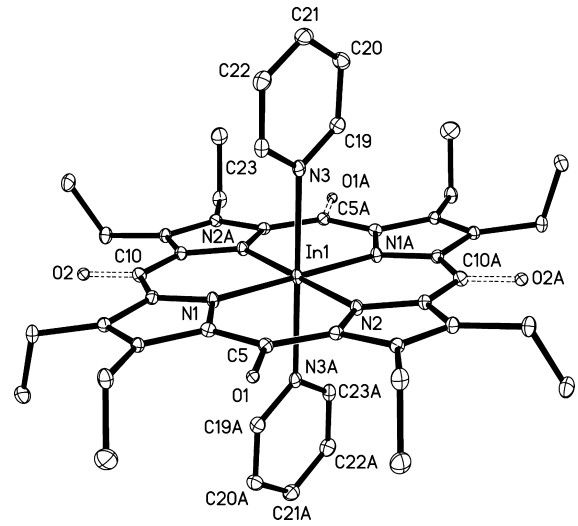

Figure 6. Drawing of the centrosymmetric $(py)_2In^{III}(OEPO)$ molecule with 30% thermal contours. Selected bond distances (Å): In1−N1, 2.1203(18); In1−N2, 2.1204(18); In1−N3, 2.4065(19); C5−O1A, 1.293(5). Selected bond angles (deg): N1−In1−N3, 91.43(7); N2−In1−N3, 88.78(7).

crystal structures frequently show hydrogen bonding to the coordinated imidazole portion of a histidine residue.[22] Model studies have demonstrated the effect of external hydrogen bonding on the stability of the metal−imidazole bond.[23] Hydrogen bonding to axial imidazole ligands appears to alter the relative ligand orientation[24] and can alter the electronic and geometric structures of five-coordinate iron(II) porphyrins.[25]

(22) Zarić, S. D.; Popović, D. M.; Knapp, E.-W. *Biochemistry* **2001**, *40*, 7914.
(23) Balch, A. L.; Watkins, J. J.; Doonan, D. J. *Inorg. Chem.* **1979**, *18*, 1228.
(24) Hu, C.; Noll, B. C.; Schulz, C. E.; Scheidt, W. R. *Inorg. Chem.* **2006**, *45*, 9721.
(25) Hu, C.; Noll, B. C.; Piccoli, P. M. B.; Schultz, A. J.; Schulz, C. E.; Scheidt, W. R. *J. Am. Chem. Soc.* **2008**, *130*, 3127.

$In\{(im)_2In^{III}(OEPO\cdots im)\}_2\cdot(im)_2In^{III}(OEPO)\cdot 2Cl_2C_6H_4$, there is hydrogen bonding between the coordinated imidazole and a second, uncoordinated imidazole as seen in Figure 5. Additionally, in this structure there is hydrogen bonding between a coordinated imidazole and the meso oxygen atom of another $(OEPO)^{3-}$ ligand. The hydrogen-bonding network that connects the molecules in $\{(im)_2In^{III}(OEPO\cdots im)\}_2\cdot(im)_2In^{III}(OEPO)\cdot 2Cl_2C_6H_4$ is related to the hydrogen-bonded pattern seen previously for $(im)_2Fe^{III}(OEPO)\cdot 2THF$ and $(im)_2Fe^{III}(OEPO)\cdot 1.6CHCl_3$.[10] In these two six-coordinate iron complexes, each meso oxygen atom of the macrocycle forms hydrogen bonds to the H−N groups of the axial ligands of two neighboring $(im)_2Fe^{III}(OEPO)$ molecules.

Experimental Section

Materials. Octaethylporphyrin (H_2OEP) was purchased from Frontier Scientific and used without further purification. Octaethyloxophlorin (H_2OEPOH) was prepared by a known route.[26]

Preparation of $\{In^{III}(OEPO)\}_2$. A green solution of 0.040 g (0.14 mmol) of indium(III) chloride, 0.250 g (3.1 mmol) of sodium acetate, and 0.070 g (0.13 mmol) of H_2OEPOH in 100 mL of acetic acid was heated under reflux for 2 h. During the heating, the solution turned magenta red. The solution was cooled and carefully neutralized with 400 mL of a saturated aqueous solution of sodium hydrogen carbonate. Neutralization produced a green solution, which was extracted with 100 mL of chloroform. The chloroform solution was washed with four 250 mL portions of water and subsequently dried over sodium sulfate. After filtration, the brown-green chloroform solution was evaporated to dryness. The brown product was recrystallized from a minimum amount of dichloromethane and methanol: yield 0.035 g (85%). MS: found, 1324.53 amu; calcd, 1324.50 amu. UV/vis for $\{In^{III}(OEPO)\}_2$ [λ_{max}, nm (ϵ, M^{-1} cm^{-1})]: 427 (6.4×10^4), 579 (1.2×10^4), 628 (1.2×10^4).

Preparation of $(py)_2In^{III}(OEPO)$. About 10 mg (0.0075 mmol) of $\{In^{III}(OEPO)\}_2$ was dissolved in 3 mL of chloroform to produce a brown solution. Upon the addition of 0.20 mL (2.48 mmol) of pyridine, the solution turned green. The solution was filtered and transferred to a 5-mm-outside-diameter glass tube. A 2.0 mL portion of methanol was carefully layered over the green solution. Upon standing for 4 weeks, deep-green crystals of the product formed. The product was collected by decantation and washed with methanol (yield 95%). UV/vis in pyridine [λ_{max}, nm (ϵ, M^{-1} cm^{-1})]: 437 (6.7×10^4), 538 (8.3×10^3), 638 (1.3×10^4), 694 (4.4×10^4).

Preparation of $\{(im)_2In^{III}(OEPO\text{-}im)\}_2\cdot(im)_2In^{III}(OEPO)\cdot 2Cl_2C_6H_4$. A 1.0 mg (0.00075 mmol) portion of $\{In^{III}(OEPO)\}_2$ was dissolved in 2.0 mL of 1,2-dichlorobenzene to form a brown solution. After the addition of 2 mg (0.029 mmol) of imidazole, the solution turned green. This solution was filtered and allowed to stand undisturbed. After 6 weeks, dark-green plates of $\{(im)_2In^{III}(OEPO\cdots im)\}_2\cdot(im)_2In^{III}(OEPO)\cdot 2Cl_2C_6H_4$ were obtained in 10% yield. UV/vis in dichloromethane with excess imidazole [λ_{max}, nm (ϵ, M^{-1} cm^{-1})]: 435 (6.5×10^4), 541 (8.2×10^3), 638 (1.4×10^4), 694 (3.3×10^4).

Physical Measurements. Electronic absorption spectra were recorded using a Hewlett-Packard 8450A diode array spectrophotometer. ^1H NMR spectra were recorded at 600 MHz at ambient temperature with $CDCl_3$ or C_5D_5N as solvents. Chemical shifts are reported in parts per million, relative to $CDCl_3$ (^1H NMR, δ 7.26) or C_5D_5N (^1H NMR, δ 8.72). The mass spectrum was acquired in the positive ion mode on an Applied Biosystems 4700 MALDI TOF/TOF.

X-ray Crystallography and Data Collection. The crystals were removed from the glass tubes in which they were grown together with a small amount of mother liquor and immediately coated with a hydrocarbon oil on the microscope slide. Suitable crystals were mounted on glass fibers with silicone grease and placed in the cold dinitrogen stream of a Bruker SMART Apex II diffractometer with graphite-monochromated Mo Kα radiation at 90(2) K. Crystal data are given in Table 1. The structures were solved by direct methods and refined using all data (based on F^2) using the software of *SHELXTL 5.1*. A semiempirical method utilizing equivalents was employed to correct for absorption.[27] Hydrogen atoms were located in a difference map, added geometrically, and refined with a riding model.

Acknowledgment. We thank the NIH (Grant GM-26226 to A.L.B.) for support.

Supporting Information Available: X-ray crystallographic files in CIF format for $\{(im)_2In^{III}(OEPO\cdots im)\}_2\cdot(im)_2In^{III}(OEPO)\cdot 2Cl_2C_6H_4$ and $(py)_2In^{III}(OEPO)$. This material is available free of charge via the Internet at http://pubs.acs.org.

IC801605B

(26) Balch, A. L.; Koerner, R.; Latos-Grazynski, L.; Lewis, J. E.; St Claire, T. N.; Zovinka, E. P. *Inorg. Chem.* **1997**, *36*, 3892.

(27) *SADABS 2.10*: Sheldrick, G. M. *Acta Crystallogr., Sect. A* **1995**, *A51*, 33, based on a method of R. H. Blessing.